Earliest Events in Protein Folding: Submicrosecond Secondary Structure Formation in Reduced Cytochrome *c*[†,‡]

Eefei Chen, Robert A. Goldbeck,* and David S. Kliger*

Department of Chemistry and Biochemistry, University of California, Santa Cruz, California 95064

Received: January 8, 2003; In Final Form: April 11, 2003

Protein folding is uniquely characterized as a dynamic process by the tremendous conformational heterogeneity of the unfolded state. This conformational heterogeneity implies the possibility of significant kinetic heterogeneity in the folding dynamics, yet many folding reactions appear to proceed homogeneously, i.e., from unfolded conformations that are in equilibrium with each other and a transition state. At what point in time on the way to the folded state the kinetic heterogeneity of the unfolded state is lost to conformational equilibration has been an open question. We present evidence in this regard obtained from nanosecond far-UV optical rotatory dispersion spectroscopy of the fastest folding process observed in photoreduced cytochrome *c*, a secondary structure formation process proceeding on a submicrosecond time scale at high denaturant concentration (observed as a "burst" phase in millisecond stopped-flow circular dichroism studies). The kinetics of this fast folding process imply that it proceeds from a conformational ensemble that is not in equilibrium with the bulk of protein conformers during the time required to completely reduce the sample, $\sim$100 μs. We thus determine a lower limit on the time required for conformational equilibration of $\sim 10^{-4}$ s, in agreement with the previous estimate from time-resolved magnetic circular dichroism measurements on photolyzed cytochrome *c*-CO (Goldbeck, R. A.; Thomas, Y. G.; Chen, E.; Esquerra, R. M.; Kliger, D. S. *Proc. Natl. Acad. Sci.* **1999**, *96*, 2782−2787). Combined with an upper limit from stopped-flow measurements (Lyubovitsky, J. G.; Gray, H. B.; Winkler, J. R. *J. Am. Chem. Soc.* **2002**, *124*, 5481−5485), this allows us to bracket the conformational diffusion time, i.e., the time interval over which the kinetic heterogeneity of this protein's unfolded state is lost through conformational equilibration, within the range $\sim 10^{-4}$−10^{-3} s. This estimate of the conformational diffusion time implies that the earliest folding events, helix formation and possibly the collapse of extended conformations, proceed under an energy landscape regime wherein conformational diffusion is slow, whereas the final (milliseconds) folding phase proceeds along a classical kinetic pathway.

Introduction

The earliest events in protein folding are of central importance in understanding how the vast number of possible conformations available to an unfolded protein can evolve to the native fold on a physiologically useful time scale. It has long been clear that the search through conformational space for the folded state cannot be random in the sense that it would be equally likely to examine all possible values of the microscopic degrees of freedom; rather, it must be limited or directed by information encoded in the sequence.[1] For instance, the sequence may encode a funnel in the free energy landscape that biases diffusion of unfolded conformations to the native conformation.[2] Alternatively, from a more traditional point of view, it may encode a kinetic pathway (or pathways).[3] If this pathway (or pathways) involves structural intermediates, then a mechanism in the conventional sense familiar from small molecule kinetics is further implied.[4]

These two views can be considered limiting cases of a more general continuum. Where the folding of a particular protein lies on this continuum depends on the roughness of the landscape determining the characteristic time for conformational diffusion relative to the height of any free energy barrier that more globally limits the folding rate. Barriers of the latter type are thought to arise frequently in the folding of proteins because loss of configurational entropy is compensated relatively late along the folding reaction coordinate by the energy released in interresidue contacts. If conformational diffusion is very fast compared to passage over such a barrier, then the unfolded conformations will be in equilibrium with each other and the transition state. In that case, transition state theory (albeit modified to account for diffusive rather than impulsive passage over the free energy saddle point) is applicable and conventional kinetic analyses in terms of pathways and intermediates are meaningful. However, if conformational diffusion is much slower than this limit, then heterogeneity arising from unequilibrated unfolded conformations can lead to kinetic complexity that may be difficult to describe in terms of pathways.

It may be further possible for both limits to operate during the folding of a given protein, but on different time scales. The earliest folding events may precede full equilibration of the unfolded conformations and thus fall within the energy landscape−conformational diffusion limit. The final folding events, on the other hand, may follow equilibration of the unfolded conformations and thus be well described by a simple two-state (or *n*-state, in the case of $n - 2$ populated intermediates) pathway.

[†] Part of the special issue "A. C. Albrecht Memorial Issue".

[‡] This paper is dedicated to the memory of Andreas C. Albrecht. As a scientist, teacher, and human being he was an inspiration for us all.

* To whom correspondence should be addressed. Fax: (831) 459-2935. E-mail: goldbeck@chemistry.ucsc.edu; kliger@chemistry.ucsc.edu.

10.1021/jp030006l CCC: $25.00
Published on Web 06/06/2003

The folding reactions of cytochrome *c* appear to offer a particular example of the latter mixed scenario, as discussed further below. However, before considering the specific case of cytochrome *c*, we point out that this scenario may be expected to occur more generally in the folding of proteins because the time scale for conformational diffusion of polypeptide chains, e.g., $\sim 10^{-4}-10^{-3}$ s for cytochrome *c*,[5,6] appears to lie roughly at the logarithmic midpoint of the time scales typically observed in protein folding. These range from $\sim 10^{-7}$ s for helix formation[7] to $\sim 10^{0}$ s for the consolidation of native secondary and tertiary structure in the final folded state. Thus the earliest appearance of secondary structure could be expected from this point of view to occur on an at least partially "frozen" landscape wherein disparate conformations of the unfolded polypeptide chain are not necessarily in kinetic communication, whereas milliseconds-to-seconds folding reactions will probably be well described by conventional kinetic pathways.

We examine in the present work new experimental evidence for the earliest folding reactions in reduced cytochrome *c* and assess its implications, both for the general picture of folding outlined above and for models of folding in terms of pathways and mechanisms that have been advanced for this protein in particular. We use nanosecond optical rotatory dispersion (TRORD) spectroscopy to monitor folding kinetics as a function of guanidine hydrochloride (GuHCl) denaturant concentration after the rapid reduction of cytochrome *c* by photoinduced electron transfer from NADH. We are thus able to resolve the "burst" phase formation of secondary structure, so-called because it is complete within the ~1-ms dead time typical in denaturant mixing studies of folding kinetics.

We find that the rise time (1/*e* formation time) of early secondary structure is significantly faster at all of the denaturant concentrations studied than the approximately hundred microsecond time scale previously believed to mark the earliest folding events in cytochrome *c*.[8,9] Moreover, we observe that the early kinetics varies with the driving force in a way that seems inconsistent with a productive, "on-pathway" folding process. Both of these observations call into question previous attempts to link the burst-phase appearance of secondary structure with conventional mechanistic pathways for folding.

Materials and Methods

Sample Preparation. Horse heart cytochrome *c* (cyt *c*) and NADH (both from Sigma), ultrapure GuHCl (ICN Biochemicals), sodium phosphate (NaP: monobasic, Na_2HPO_4, and dibasic, NaH_2PO_4; Fisher Scientific) and sodium hydrosulfite (dithionite, Fluka) were used as purchased. The samples for time-resolved experiments were made by first preparing ~75 μM cyt *c* in buffer solutions containing 0.1 M NaP with either 2.7 (pH 7.0), 3.0 (pH 7.1), 3.3 (pH 7.1), or 4 M (pH 7.1) GuHCl. The cyt *c* solution was then stirred in air for approximately 15 min before it was deoxygenated with argon gas for 15−30 min. This step helped to oxidize any traces of reduced cytochrome *c* (redcyt *c*), which was detected in concentrations as high as 10% in oxidized cytochrome *c* (oxcyt *c*) solutions before stirring in air. The oxygen-free cyt *c* solution was then added to a separately deoxygenated vial containing solid NADH (~500 μM). The protein sample was placed into a glovebag that was continuously purged with nitrogen or argon gas. The glovebag also contained a peristaltic pump that was used to flow the sample to and from a 1.3-mm path length sample cell with fused silica windows.

Time-Resolved Experiments. Far-UV TRORD spectroscopy, rather than time-resolved circular dichroism (TRCD), was used to monitor secondary structure formation in the present study primarily because ORD experiments can provide higher signal-to-noise data for measurements where light intensities are low due to high sample absorbance. The CD signals that are characteristic of protein secondary structure are localized to the far-UV absorption bands and show a rapid decrease away from the absorption maximum. In contrast, the contribution of this transition to the ORD signal decreases much more gradually in spectral regions removed from the absorption maximum. Thus, ORD signals can be measured outside the absorption bands, giving a signal-to-noise advantage, particularly in measurements that are limited by the probe intensity.

Transfer of an electron from NADH to oxcyt *c* was initiated with 7-ns, 36-mJ pulses of 355-nm light from a Quanta Ray DCR-1 Nd:YAG laser. Spectral changes induced by the electron-transfer event were probed with white light from a xenon flash lamp. The ~7 mm × 5 mm cross section excitation beam entered the sample cell at an angle of 30° from normal, overlapping the 300-μm-diameter probe beam propagating normal to the sample face. Details of the TRORD measurements have already been published and will be described only briefly here.[10] The sample cell is placed between two MgF_2 polarizers oriented nearly perpendicularly to each other (near-crossed position). The first polarizer is rotated by a small angle $\pm\beta$ from the crossed position relative to the analyzing polarizer. (In these experiments, $\beta = 1.87°$; in general, $|OR_{sample}| \ll \beta \ll 90°$.) After passing through the polarizers and sample, the probe beam is focused onto the slit of a spectrograph, dispersed by a 600 grooves/mm grating blazed at 200 nm, and detected by a gated optical multichannel analyzer (OMA). The difference between the signal measured at $+\beta$ and $-\beta$ is proportional to the ORD.

TRORD data for cyt *c* at each concentration of GuHCl were obtained at 25 time delays ranging from 320 ns to 800 ms after initiation of folding, using a 400-ns sampling gate centered around the nominal delay time. A total of 1500−2000 averages were collected at each of the four time points between 320 ns and 1 μs, and 800−1000 averages were obtained at each of the time points remaining from 2 μs to 800 ms. Data were collected with a 2-s delay between each laser flash. Sample flow at a rate of 8 μL/s between laser flashes moved the irradiated sample volume out of the pump−probe path before the next laser pulse and avoided the buildup of photoreduction and photodegradation products. The sample temperature was maintained at 24−25 °C, measured with an infrared temperature probe (Fluke 80T-IR, Fluke Corporation, Everett, WA). The cyt *c* sample was recycled between the flow cell and the sample reservoir. Its UV−vis spectrum (UV-2101PC Shimadzu spectrophotometer) was checked frequently for signs of redcyt *c* buildup by comparison with the spectrum of the oxcyt *c* sample measured before laser irradiation. The GuHCl concentrations in the pure buffer and in the oxcyt *c* solutions before and after the experiments were measured on a refractometer (ABBE-3L Milton Roy Company, Rochester, New York). The pH values of the oxcyt *c* solutions were also measured before and after the experiments.

Data Analysis. The TRORD data were analyzed as the difference of the photoproduct and the initial state spectrum of oxcyt *c*. Singular value decomposition (SVD) and global kinetic analyses were performed on the multiwavelength ORD data (Figure 1), as well as on the kinetic trace (Figure 2) that was obtained from the ORD data by averaging the signals in a 6-nm region around 230 nm. (Note that due to a reoxidation artifact, discussed below, the three longest time points measured were omitted from the kinetic fitting for each denaturant concentra-

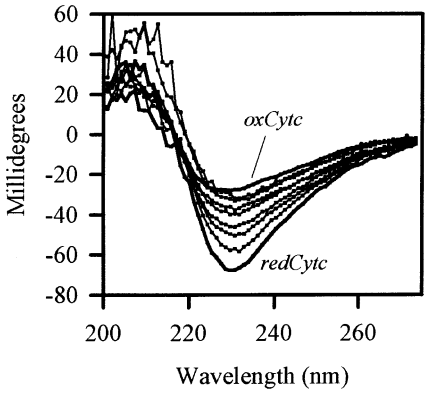

Figure 1. Far-UV TRORD monitors secondary structure formation during folding of reduced cytochrome *c* prepared from unfolded oxidized protein by rapid photooxidation of NADH. Dispersions measured at 820 ns, 10 μs, 1 ms, 50 ms, 100 ms, 200 ms, and 500 ms after phototriggering have increasingly negative extrema with longer time delays (dotted lines). The equilibrium spectra of the initial state (oxcyt *c*) and the final state (redcyt *c*) are represented by solid black lines. (Features below 215 nm such as the positive 205-nm band have very low signal-to-noise ratios because of light absorption by GuHCl.) The starting material, 75 μM oxcyt *c*, was prepared in 0.1 M NaP, 2.7 M GuHCl, and 500 μM NADH at pH 7. Equilibrium redcyt *c* was prepared by adding dithionite to a portion of the oxcyt *c* solution. All spectra were measured at 25 °C in a 1.3-mm path length cell.

tion.) The algorithms for the analyses were written with the mathematical software package Matlab (Pro-Matlab, The Math Works, Inc., South Natick, MA). Readers are directed to previously published details of SVD and global analyses that are discussed with respect to heme proteins[11] and to far-UV TRCD studies.[12] All percentage and fractional yields of secondary structure formation discussed below were calculated from the TRORD photolysis difference at 230 nm relative to the difference between dithionite reduced protein and oxidized starting material measured at the appropriate denaturant concentration.

Results

The negative ORD extremum at 230 nm, corresponding mainly to the OR contributions of the lowest energy peptide n $\rightarrow \pi^*$ transitions of residues located in regions of helical secondary structure, increased in magnitude after NADH photoreduction of the heme triggered the protein to fold. Seven representative time points from the 25 TRORDs measured at 2.7 M GuHCl are shown in Figure 1, along with the equilibrium ORD of oxcyt *c* and redcyt *c*. The changes in the ORD signal observed after photoinitation of folding were interpreted as the formation of protein secondary structure because they are similar to the ORD of (folded) redcyt *c* in band shape and sign. The increase in the 230-nm TRORD magnitude occurs in two broad temporal phases: a fast phase in the microsecond time regime (identified with the stopped-flow burst phase) and a slow phase with a time constant of hundreds of milliseconds (Figure 2). The characteristic time constants and amplitudes for both phases were observed to depend on denaturant concentration (Table 1). TRORD measurements after photoexcitation of cyt *c* samples in the absence of NADH showed no significant dynamics (see Figure 2C), demonstrating that the secondary structure changes observed in the presence of NADH were a result of photoinitiated electron transfer from NADH to the heme.

Comparison with TRCD. Because TRORD and TRCD spectroscopy both probe the dynamics of secondary structural changes, the two techniques are expected to yield similar kinetic

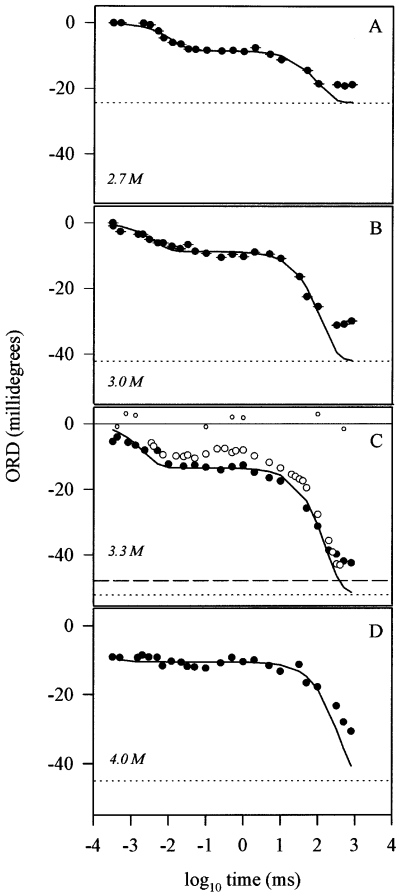

Figure 2. (A−D) Increasing denaturant concentration shortens the rise time of the submillisecond TRORD signal during NADH photooxidation triggered folding. Photoreduced-folding minus initial state TRORD difference signals (filled circles) averaged over a 6-nm interval around 230 nm and equilibrium reduced minus oxidized ORD difference values (dotted line) are shown in panels A−D for the following GuHCl concentrations: (A) 2.7, (B) 3.0, (C) 3.3, and (D) 4.0 M. Solid lines overlaying the data points show the two-exponential fits reported in Table 1. For comparison, the TRCD signal averaged around 222 nm (ref 13) measured under similar conditions is shown in panel C (large open circles) with the equilibrium reduced minus oxidized CD value (dashed line) as is the TRORD signal observed in the absence of NADH (small open circles). All other conditions are as in the Figure 1 legend.

TABLE 1: Observed Lifetimes from Far-UV TRORD Measurements of NADH-Photoreduced Cytochrome *c* Folding vs Guanidine Hydrochloride Denaturant Concentration[a,b]

[GuHCl], mol/L	τ_1, μs	τ_2, ms
2.7	12 ± 2 (0.35)	100 ± 10 (0.65)
3.0	5 ± 3 (0.21)	120 ± 20 (0.79)
3.3	2.2 ± 0.5 (0.26)	160 ± 10 (0.74)
4.0	≤0.4 (0.23)	380 ± 30 (0.77)

[a] Conditions: 0.1 M sodium phosphate buffer, pH 7, ~500 μM NADH, 25 °C. [b] Fractional relative amplitudes in parentheses.

results for this system. A comparison of the TRCD data previously published for this system with the TRORD data measured in the present study under the same conditions shows that their time evolutions are indeed very similar (see Figure 2C).[13,14] (A slight retrograde time evolution in the TRCD signal between 100 μs and 1 ms may suggest a small amplitude helix unwinding process,[13] but such a retrograde evolution is not apparent in the TRORD data for 3.3 M GuHCl. It is possible that the more spectrally localized TRCD data are more sensitive at 220 nm to this process than are the 230-nm TRORD data.)

Fast Folding Phase. The fast folding phase of redcyt *c* ($t \ll 1$ ms) shows new and interesting folding kinetics as a function of GuHCl concentration. The most striking new feature of the folding dynamics of cyt *c* is found in 4.0 M GuHCl, wherein a large increase in negative optical rotation is observed to form within several hundred nanoseconds (see Figure 2D). The rise time of this ultrafast secondary structure formation appears to slow considerably with lower denaturant concentration, however, becoming about 12 μs at the lowest GuHCl concentration studied, 2.7 M (see Figure 2A).

Interestingly, the reduction kinetics of cyt *c*, as assessed by time-resolved Soret band absorption measurements (data not shown), are insensitive to GuHCl concentration over the range 2.7−4.0 M, in contrast to the secondary structure kinetics. At each of the GuHCl concentrations used in this range, reduction was observed to be about 15, 50, and 90% complete at 0.5, 5.0, and 50 μs, respectively. We thus infer that the denaturant-dependent kinetic barrier giving rise to the observed variation in the rise time of the early ORD signal is intrinsic to the secondary structure formation process. Note that these observations imply that we were able to detect folding kinetics at the highest denaturant concentration that were much faster than the apparent half-life of the reductants used to trigger folding, a seemingly paradoxical finding that is discussed further below.

The fractional amplitude of the fast phase decreased by a factor of nearly 2 when the denaturant concentration was increased from 2.7 to 4.0 M. However, this observation actually represented a nearly constant magnitude in the absolute signal. This is because the fractional amplitude was normalized to the static difference between oxidized and reduced protein ORD signals, which doubled over this concentration range, as explained further below.

Slow Folding Phase. The time constant of the large amplitude, slow folding phase approximately doubled as the GuHCl concentration was increased from 2.7 to 4.0 M (see Table 1). This process is associated with the formation of native secondary structure,[13] with native Met-His heme ligation, as a nonnative His ligand is displaced by Met 80.[15,16] Previous studies have determined that the activation energy of this process has a linear free energy dependence on the change in folding stability induced by GuHCl denaturant ($\alpha \sim 0.4$),[17] a dependence that is consistent with the variation observed here.

The amplitude of the slow process also increased with denaturant concentration. However, we attribute this not to an increase in the formation of secondary structure in the final folded state, as the latter is expected to form completely at all the denaturant concentrations studied, but rather to a decrease in secondary structure content of the starting material. At 2.7 M GuHCl, the oxidized starting material comprises ~50% fully unfolded conformations and ~50% compact nonnative forms containing disordered tertiary structure and nativelike secondary structure.[18] The oxcyt *c* secondary structure content drops sharply from this composition as the protein cooperatively unfolds with increasing denaturant concentration, becoming negligible by 3.3 M GuHCl, a trend that is reflected in the equilibrium ORD of the starting material (Figure 3). The concomitant change in net secondary structure formation accounts for the trend in fractional amplitudes observed in Table 1 on going from 2.7 to 4.0 M GuHCl. As the net formation of secondary structure doubles over this concentration range, the fractional amplitude of the (constant absolute magnitude) fast process decreases by a factor of nearly 2 and the amplitude of the slow process increases concomitantly.

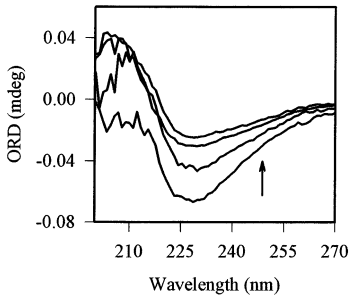

Figure 3. Equilibrium ORD of the oxidized cytochrome *c* starting material measured at 2.7, 3.0, 3.3, and 4.0 M GuHCl, respectively (arrow indicates direction of increasing GuHCl concentration). Sample conditions as in Figure 1 legend.

The amount of secondary structure actually observed to form by 1 s in the TRORD experiments, the longest time delay at which data were measured, was limited to about 75% of the difference between native redcyt *c* and denatured oxcyt *c* (see Figure 2). At least two factors probably contributed to the smaller than expected yield of secondary structure. First, as the concentration of GuHCl increases, it is expected that complete folding will take longer than 1 s. This is evident in the increasing observed time constants for the final folding process with increasing GuHCl concentration. Second, it is necessary to consider competition from reoxidation of redcyt *c* by the presence of small amounts of adventitious oxygen. Because the cyt *c* solutions were extensively deoxygenated before the measurements, the extent of reoxidation probably depended mainly on the oxygen permeability of the sample cell. A small but finite oxygen permeability of the TRORD sample cell presumably accounts for the small reoxidation of sample observed at the longest times. Similarly, the difference observed in the final percentages of folded structure in the present TRORD and the previous TRCD experiments (see Figure 2C) may be due at least in part to differences in oxygen permeability for the different sample cells used in the ORD and CD studies. In any event, the fast folding phase, the primary focus of the present study, does not appear to be affected by the slow reoxidation process.

Discussion

Studies of early intermediates of folding in cyt *c* and other small proteins have been motivated by their possible connections to pathways and mechanisms of folding.[19] One of the earliest folding events observed in cyt *c* appears to involve collapse of the unfolded chains to more compact conformations, as indicated by the quenching of Trp 59 fluorescence via energy transfer to the heme.[6,9] Measured time constants for collapse lie in the 50−100 μs range and depend weakly on the denaturant concentration. Furthermore, from the burst phase signal observed to develop within the ~1 ms dead time of previous stopped-flow far-UV CD studies, it is known that some secondary structure formation also takes place on the submillisecond time scale in cyt *c*. Because of the 400-μs dead time limiting the time resolution of mixed flow CD studies, however, it has not been clear whether the appearance of this early secondary structure coincides with the collapse process.[20]

The question of the relative time scales of early secondary structure formation and collapse has potentially significant implications for folding mechanisms. In the framework model, for instance, elements of native secondary structure form first and provide a framework that facilitates the appearance of native tertiary contacts.[3b,21] The nucleation model also starts with the appearance of some element of native secondary structure,

although in that model it is localized to a nucleus that then facilitates formation of the remaining native state structure without the appearance of populated intermediates.[22] In the hydrophobic collapse model, on the other hand, collapse gives rise to tertiary structure that facilitates the formation of native secondary structure.[23]

We use nanosecond TRORD spectroscopy to examine in the present work the question of the rise time for the early secondary structure formation phase (burst phase) of cytochrome *c*. Our recent TRCD study of this system found an apparent rise time of several microseconds,[13] significantly faster than the collapse process previously identified as the fastest observable process in the folding reactions of this protein.[8,9] However, because the time constant measured in the TRCD study was similar to the rise time of the heme photoreduction process ($t_{1/2} = 5\ \mu$s) used to trigger folding,[24] it was not clear if the kinetics observed there were limited by folding or reduction. In either case, we can conclude that the early secondary structure rise time is faster than that previously observed for collapse in denaturant dilution and temperature jump studies of the oxidized protein, ~100 μs.[6,9] However, the question remained, is it faster than the photoreduction trigger? The present work attempts to resolve this point by studying the rise time as a function of denaturant concentration.

Photochemical methods to rapidly trigger folding reactions in cyt *c* use changes in the ligation or oxidation state of the heme to shift the folding equilibrium. Folding titration curves, measured using both fluorescence and CD probes, show that redcyt *c* is more folded than the oxidized protein in the 2−5 M GuHCl concentration range.[18,24,25] Similarly, the carbon monoxide bound (cyt *c*-CO) reduced state is less stable to folding than the CO-unbound form. Thus folding of redcyt *c* can be triggered rapidly by either laser-induced electron injection[24,26] or ligand photodissociation processes,[25] wherein reduction of unfolded oxcyt *c* or photolysis of the Fe(II)−CO bond in cyt *c*-CO, respectively, destabilizes the unfolded conformations relative to the folded state of the protein. The CO photodissociation event is extremely rapid, which would seem to make it an ideal fast folding trigger, but the photolyzed CO recombines with heme before much folding can occur (~10% native secondary structure formation is detected at 2 μs after photodissociation[27]). The CO method has been most useful for studying heme-residue binding reactions as a probe of the conformational dynamics of the unfolded chains on the folding energy landscape.[5,28] In this regard, time-resolved optical absorption (TROA) experiments on photolyzed cyt *c*-CO identified a 40-μs species attributed to the formation of bis-His heme ligation and a faster process with an observed time constant of several microseconds attributed to the formation of a small fraction of natively ligated conformers,[25,27] assignments that have been confirmed by more ligand-sensitive time-resolved magnetic circular dichroism (TRMCD) measurements.[5]

The photoreduction method, on the other hand, uses an irreversible reaction that allows the entire time course of the folding reaction to be studied. However, a disadvantage of this approach is that the triggering reactions are second order and require about 100 μs to reach completion, a time scale that overlaps with the early folding events of cyt *c*. Furthermore, the trigger is heterogeneous in that at least two strong reducing species are generated by photoexcitation of NADH, solvated electrons, and NAD$^\bullet$ radicals.[26]

To overcome the limitations of the photoreduction method, we took advantage of the observation that the driving force for folding could be varied by changing the denaturant concentration, without changing the reduction kinetics. The resulting increase observed in the time required for the slow folding phase at high denaturant concentration was expected from the known linear dependence of its activation energy on the folding free energy. The striking variation in the observed time constant for the fast phase, on the other hand, is surprising for two principal reasons.

First, given that the overall time scale for reduction is similar to that observed in the fast TRORD signal, one would not expect to observe dramatic changes in the latter signal under homogeneous conditions. Our observation of a denaturant-dependent trend in the fast TRORD time constants, the shortest being an order of magnitude smaller than the reduction $t_{1/2}$, thus implies probable heterogeneity in the protein that is in addition to the known heterogeneity of the reductants. This is because a homogeneous protein solution is expected to be rate-limited with regard to its fastest observable kinetics by the overall time constant for reduction, even in the presence of two reductants with different reduction rate constants, k_e and k_{NAD}, one of which (k_e) is expected to be much faster than the other. To see this, consider first the ideal case of the pseudo-first-order rate constant $k_1 = k_e[e^-_{aq}] + k_{NAD}[NAD^\bullet]$, which would be applicable to the reduction kinetics if e^-_{aq} and NAD$^\bullet$ were present in great excess. In that case, the reduction kinetics would be dominated by the solvated electron term in k_1, which represents the fastest route to triggering folding, and no faster folding kinetics could be directly observed. Now relax the constraint to pseudo-first-order kinetics and assume that e^-_{aq} and NAD$^\bullet$ are produced in concentrations more similar to that of cyt *c*, a scenario that is more applicable to the present NADH photoexcitation conditions. The reduction kinetics will take a more extended time course than the simple exponential evolution of the pseudo-first-order case, but any fast intramolecular protein relaxation it triggers would still be rate-limited by the reduction process. In other words, if the intramolecular process is intrinsically very rapid, its observed kinetics would merely mirror that of the overall reduction process used to trigger it. Therefore, to explain the observation here of an intramolecular time constant that is faster than that for (overall) reduction, we need to further posit that there is a special conformational subpopulation of the unfolded protein chains, one that rapidly forms secondary structure upon reduction by e^-_{aq} and that is not in equilibrium (at least on time scales less than ~100 μs) with the remaining conformations. In this case, solvated electron reductant can trigger folding reactions in the subpopulation on the submicrosecond time scale, permitting direct observation of submicrosecond folding kinetics. The reduction of the remaining (slow folding) protein conformations will not obscure observation of the fast folding kinetics because they are kinetically isolated from and cannot interconvert with the rapidly folding form. A possible physical basis for the kinetic heterogeneity inferred here for the unfolded protein conformations lies in the concept of the conformational diffusion time introduced above and discussed further below.

A schematic illustration of these ideas is presented in Figure 4, which presents very simple model calculations for two limiting cases: conformational diffusion much slower than reduction ($\tau_{diffusion} \sim 100\ \mu$s) and very rapid diffusion ($\tau_{diffusion} \sim 1$ ns). The model uses the simplest kinetic scheme (Scheme 1) embodying fast and slow reacting unfolded conformational subpopulations in the oxidized starting material, U_f^{III} and U_s^{III}, respectively, a fast-forming nonnative reduced intermediate with high (near native) helix content, I_f^{II}, the slow-reduction product U_s^{II}, and the native reduced state, N^{II}. The submicrosecond−microsecond reduction and secondary structure formation processes taking place in the U_f conformational ensembles are convoluted in the pseudo-first-order rate constant $k_1 = 3 \times 10^6$

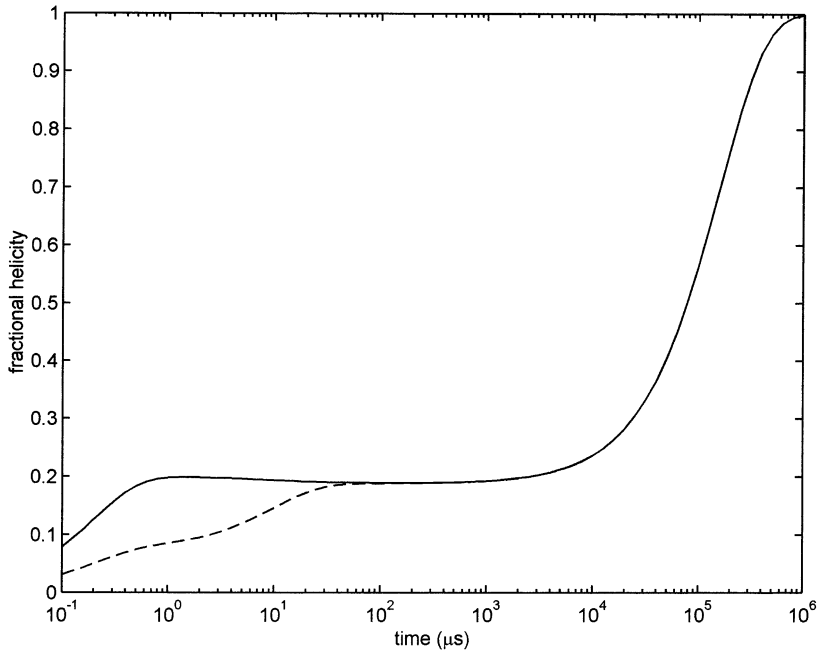

Figure 4. Model calculations of TRORD signal (represented as fractional helicity) showing homogeneous and heterogeneous folding kinetics, respectively, in the presence of fast and slow conformational equilibration of the unfolded protein chain. Conformational diffusion times: ~100 μs (—) and ~1 ns (- - -). See text for discussion.

SCHEME 1

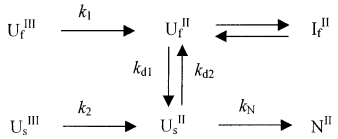

s^{-1} (for simplicity, U_f^{II} and I_f^{II} are assumed to be in a rapid 1:1 equilibrium), the slow ($\tau \sim 10$ μs) reduction of the remaining unfolded ensembles is represented by k_2, and the ~100-ms folding process producing the native state is represented by k_N. (This scheme serves merely to illustrate how slow conformational equilibration can make it possible to measure a time constant for secondary structure formation that is faster than the overall reduction kinetics, whereas the actual kinetics are expected to be much more complex. Those are expected to include conformational equilibration between U_f^{III} and U_s^{III}, second order reduction reactions with limited amounts of reductant, and the possibility of a more substantial free energy barrier between I_f^{II} and U_f^{II}.) The only parameter that is varied in Figure 4 is the conformational diffusion time, embodied by the rate constants k_{d1} and k_{d2} representing forward and backward conversion, respectively, between U_f^{II} and U_s^{II} (k_{d2} was set equal to $0.3k_{d1}$ to match the apparent ratios of the f and s ensembles in the starting material). In the slow conformational diffusion case ($k_{d1} = 1/100$ μs), the kinetics of the fractional helicity show a fast component with a submicrosecond rise time that is similar by construction to the fast rise time observed in the high denaturant TRORD data. In the rapid diffusion example ($k_{d1} =$ 1/1 ns), on the other hand, the initial rise time of the signal is limited by the time course of overall reduction, in line with intuitive expectations based on the behavior of homogeneous systems. The surprisingly fast rise times of the TRORD data at high denaturant concentrations thus suggest that conformational equilibration among the unfolded ensembles is slow compared to the earliest folding events in cytochrome *c*, resulting in the observation of heterogeneous folding kinetics on time scales less than ~100 μs.

The second surprising feature of the fast secondary structure kinetics is the decrease in observed time constant with increasing denaturant concentration. Productive folding reactions (i.e., reactions leading to the native state) in small proteins, such as the slow phase of cyt *c*, more typically show the opposite behavior. The rate constant for folding (k_f) often slows with a decrease in driving force while the unfolding rate constant (k_u) speeds up, the combined effect giving a characteristic chevron shape to semilog plots of the observed rate constant, ($k_f + k_u$), versus denaturant concentration (if the activation energies depend linearly on the reaction free energy).[4] The denaturant dependence observed here thus suggests, although it does not prove, that the fast folding phase does not produce natively folded protein. On the other hand, the similarity of the fractional amplitude for fast helix formation observed at high denaturant concentration to the fraction of protein reduced on that time scale suggests that the ensembles produced do have nativelike helix content. The N, C, and 60's helices making up the ordered secondary structure of the native state are all relatively closely tied to the heme by covalent or coordination bonds in this small protein. It thus seems plausible that submicrosecond relaxation to nativelike helical structures could be triggered in some or all of these regions by heme reduction in a subpopulation of the chain conformers, without the need for large (slow) tertiary conformational changes.

In seeking to understand the denaturant dependence of the early time kinetics, the effect of denaturant on the conformational composition of the starting material, unfolded oxcyt *c*, should also be considered as a possible factor. In the native state, the heme group of cyt *c* is axially ligated to His 18 and Met 80. However, a nonnative ligand has been shown to replace Met 80 in both oxcyt *c* and redcyt *c* with increasing concentrations of GuHCl. This nonnative ligand has been identified with His residues 33 and 26.[15,16,29,30] These bis-His forms will be the dominant ferric heme ligation forms for values of [GuHCl] above 1.5 M and thus the heme ligation composition of oxcyt *c* is not expected to vary significantly over the concentration range studied in the present work. On the other hand, the secondary structure content of the starting material is expected to vary with denaturant concentration because of the large presence mentioned above of (molten-globule-like) nonnative

compact conformations at 2.7 M GuHCl. However, these compact forms make very small or negligible contributions to the conformational distributions for concentrations within the rest of the concentration range studied, 3−4 M. It therefore seems unlikely that they are connected to the large kinetic changes observed within this range. Thus, there does not appear to be a connection between the denaturant-dependent trends in oxcyt *c* conformational composition and the fast kinetic phase beyond the indirect effect on its fractional amplitude.

From the point of view of conventional mechanistic models of folding, the conclusion advanced here and by our previous work that the early formation of secondary structure precedes collapse in cyt *c* would seem most consistent with the tenets of the framework model.[31] The (denaturant-dependent) kinetic barrier to early secondary structure formation could be interpreted in that view as leading to an intermediate containing helical structure that might provide a framework facilitating the later formation of native tertiary structure. However, such simple mechanistic interpretations must be tempered by the additional conclusion reported here that the unfolded conformational ensembles of redcyt *c* do not appear to be in full equilibrium with each other over the time interval required for reduction of the sample, ∼100 μs. This disequilibrium means that a basic assumption of the transition state theory underlying such mechanistic models, the rapid equilibration of reactant and transition states, may not be valid on this time scale.

The lack of conformational equilibrium inferred here implies that the time required to reach equilibrium is longer than the reduction time. This inequality represents a lower limit on the conformational diffusion time of $\sim 10^{-4}$ s, in agreement with our previous study of photolyzed cyt *c*-CO.[5] In that study, we inferred a similar limit on the diffusion time from an observed disequilibrium between chain conformations poising either a methionine or a histidine residue for facile binding to the vacant heme axial site. Other workers have reported that the unfolded protein conformers of cyt *c* appear to equilibrate by the end of the several millisecond dead time typical of stopped-flow denaturant dilution studies.[32] Thus, the conformational diffusion time of cyt *c*, i.e., the time characterizing loss of the kinetic heterogeneity associated with conformational heterogeneity of the unfolded state, appears to lie in the range of $10^{-4}-10^{-3}$ s.

The present study has focused on the earliest events in folding, events occurring in a time regime wherein the conformational heterogeneity of the protein backbone and its residue side chains will be greatest. It is this heterogeneity that uniquely characterizes the protein folding problem. Just when on the way to the native state the unfolded chains lose the kinetic heterogeneity implied by this conformational heterogeneity has been an open question. The results reported here suggest that conformational heterogeneity in the folding kinetics of cytochrome *c* is lost through equilibration on the hundred microsecond to millisecond time scale. These results thus add further experimental support to the idea that the folding reactions of cytochrome *c* are an example of the mixed scenario for folding described in the Introduction. This scenario bridges the energy landscape and classical views of protein folding in that the early folding events−early helix formation and possibly the collapse of extended conformations−appear to proceed under an energy landscape regime wherein conformational diffusion is slow and possibly rate limiting, whereas the slow (milliseconds) folding phase of cytochrome *c* appears to proceed along a more classical kinetic pathway.

Acknowledgment. This work was supported by National Institute of General Medical Sciences (NIH) Grant GM38549.

References and Notes

(1) Levinthal, C. *J. Chim. Phys.* **1968**, *65*, 44−45.

(2) (a) Bryngelson, J. D.; Wolynes, P. G. *Proc. Natl. Acad. Sci. U.S.A.* **1987**, *84*, 7524−7528. (b) Bryngelson, J. D.; Wolynes, P. G. *J. Phys. Chem.* **1989**, *93*, 6902−6915. (c) Dill, K. E.; Chan, H. S. *Nat. Struct. Biol.* **1997**, *4*, 10−19. (d) Chan, H. S.; Dill, K. A. *Proteins: Struct. Funct. Genet.* **1998**, *30*, 2−33. (e) Leopold, P. E.; Montal, M.; Onuchic, J. N. *Proc. Natl. Acad. Sci. U.S.A.* **1992**, *89*, 8721−8725.

(3) (a) Creighton, T. E. *Biochem. J.* **1990**, *270*, 1−16. (b) Kim, P. S.; Baldwin, R. L. *Annu. Rev. Biochem.* **1990**, *59*, 631−660. (c) Englander, S. W.; Mayne, L. *Annu. Rev. Biophys. Biomol. Struct.* **1992**, *21*, 243−265.

(4) Fersht, A. *Structure and Mechanism in Protein Science*: *A Guide to Enzyme Catalysis and Protein Folding*; W. H. Freeman: New York, 1999.

(5) Goldbeck, R. A.; Thomas, Y. G.; Chen, E.; Esquerra, R. M.; Kliger, D. S. *Proc. Natl. Acad. Sci. U.S.A.* **1999**, *96*, 2782−2787.

(6) Hagen, S. J.; Eaton, W. A. *J. Mol. Biol.* **2000**, *297*, 781−789.

(7) Gilmanshin, R.; Williams, S.; Callender, R. H.; Woodruff, W. H.; Dyer, R. B. *Proc. Natl. Acad. Sci. U.S.A.* **1997**, *94*, 3709−3713.

(8) Chan, C. K.; Hu, Y.; Takahashi, S.; Rousseau, D. L.; Eaton, W. A.; Hofrichter, J. *Proc. Natl. Acad. Sci. U.S.A.* **1997**, *94*, 1779−1784.

(9) Shastry, M. C.; Roder, H. *Nat. Struct. Biol.* **1998**, *5*, 385−392.

(10) Shapiro, D. B.; Goldbeck, R. A.; Che, D.; Esquerra, R. M.; Paquette, S. J.; Kliger, D. S. *Biophys. J.* **1995**, *68*, 326−334.

(11) (a) Henry, E. R.; Hofrichter, J. *Methods Enzymol.* **1992**, *210*, 129−192. (b) Goldbeck, R. A.; Kliger, D. S. *Methods Enzymol.* **1993**, *226*, 147−177.

(12) Chen, E.; Lapko, V. N.; Song, P.-S.; Kliger, D. S. *Biochemistry* **1997**, *36*, 4903−4908.

(13) Chen, E.; Wittung-Stafshede, P.; Kliger, D. S. *J. Am. Chem. Soc.* **1999**, *121*, 3811−3817.

(14) Although the GuHCl concentration was reported to be 3.5 M in ref 13, later recalibration of our GuHCl analysis method corrected this value to 3.3 M.

(15) Elöve, G. A.; Bhuyan, A. K.; Roder, H. *Biochemistry* **1994**, *33*, 6925−6935.

(16) Colón, W.; Wakem, L. P.; Sherman, F.; Roder, H. *Biochemistry* **1997**, *36*, 12535−12541.

(17) Mines, G. A.; Pascher, T.; Lee, S. C.; Winkler, J. R.; Gray, H. B. *Chem. Biol.* **1996**, *3*, 491−497.

(18) Thomas, Y. G.; Goldbeck, R. A.; Kliger, D. S. *Biopolymers* **2000**, *57*, 29−36.

(19) Roder, H.; Colon, W. *Curr. Opin. Struct. Biol.* **1997**, *7*, 15−28.

(20) Akiyama, S.; Takahashi, S.; Ishimori, K.; Morishima, I. *Nat. Struct. Biol.* **2000**, *7*, 514−520.

(21) (a) Ptitsyn, O. B. *Dokl. Akad. Nauk. SSSR* **1973**, *210*, 1213−1215. (b) Bashford, E.; Cohen, F. E.; Karplus, M.; Kuntz, I. D.; Weaver, D. L. *Proteins*: *Struct. Funct. Genet.* **1988**, *4*, 211−227. (c) Karplus, M.; Weaver, D. L. *Protein Sci.* **1994**, *3*, 650−668.

(22) (a) Wetlaufer, D. B. *Proc. Natl. Acad. Sci. U.S.A.* **1973**, *70*, 697−701. (b) Wetlaufer, D. B. *Trends Biochem. Sci.* **1990**, *15*, 414−415.

(23) (a) Ptitsyn, O. B. *Trends Biochem. Sci.* **1995**, *20*, 376−379. (b) Kuwajima, K. *Proteins*: *Struct. Funct. Genet.* **1989**, *6*, 87−103.

(24) Pascher, T.; Chesick, J. P.; Winkler, J. R.; Gray, H. B. *Science* **1996**, *271*, 1558−1560.

(25) Jones, C. M.; Henry, E. R.; Hu, Y.; Chan, C.-K.; Luck, S. D.; Bhuyan, A.; Roder, H.; Hofrichter, J.; Eaton, W. A. *Proc. Natl. Acad. Sci. U.S.A.* **1993**, *90*, 11860−11864.

(26) Telford, J. R.; Wittung-Stafshede, P.; Gray, H. B.; Winkler, J. R. *Acc. Chem. Res.* **1998**, *37*, 755−763.

(27) Chen, E.; Wood, M. J.; Fink, A. L.; Kliger, D. S. *Biochemistry* **1998**, *37*, 5589−5598.

(28) (a) Hagen, S. J.; Hofrichter, J.; Eaton, W. A. *J. Phys. Chem. B* **1997**, *101*, 2352−2365. (b) Hagen, S. J.; Latypov, R. F.; Dolgikh, D. A.; Roder, H. *Biochemistry* **2002**, *41*, 1372−1380.

(29) Babul, J.; Stellwagen, E. *Biopolymers* **1971**, *10*, 2359−2361.

(30) Other nonnative ligands, such as the N-terminal amino group or lysine, may also be observed under different conditions. See: (a) Hammack, B.; Godbole, S.; Bowler, B. E. *J. Mol. Biol.* **1998**, *275*, 719−724. (b) Russell, B. S.; Melenkivitz, R.; Bren, K. L. *Proc. Natl. Acad. Sci. U.S.A.* **2000**, *97*, 8312−8317. (c) Tezcan, F. A.; Winkler, J. R.; Gray, H. B. *J. Am. Chem. Soc.* **1999**, *121*, 11918−11919. Note, however, that the terminal NH_2 group is acetylated in cyt *c* isolated from horse heart and cannot bind to the heme.

(31) A caveat to this conclusion is that observations of collapse have been made on oxcyt *c*, whereas the current observations apply to redcyt *c*. We are thus assuming that the two oxidation states of the protein have similar dynamics for both the collapse and fast secondary structure processes when under the same driving force, as is known to be the case for the slow folding phase.

(32) (a) Lyubovitsky, J. G.; Gray, H. B.; Winkler, J. R. *J. Am. Chem. Soc.* **2002**, *124*, 5481−5485. (b) Lee, J. C.; Chang, I. J.; Gray, H. B.; Winkler, J. R. *J. Mol. Biol.* **2002**, *320*, 159−164.